Eur. Phys. J. C 27, 229–241 (2003)
Digital Object Identifier (DOI) 10.1140/epjc/s2002-01099-8

THE EUROPEAN PHYSICAL JOURNAL C

Gluon condensate in charmonium sum rules with three-loop corrections

B.L. Ioffe[a], K.N. Zyablyuk[b]

Institute of Theoretical and Experimental Physics, B.Cheremushkinskaya 25, Moscow 117218, Russia

Received: 16 July 2002 / Revised version: 6 November 2002 /
Published online: 24 January 2003 –

Abstract. Charmonium sum rules are analyzed with the primary goal to obtain the restrictions on the value of the dimension 4 gluon condensate. The moments $M_n(Q^2)$ of the polarization operator of the vector charm currents are calculated and compared with the experimental data. The three-loop (α_s^2) perturbative corrections, the contribution of the gluon condensate with α_s corrections and the contribution of the dimension 6 operator G^3 are accounted. It is shown that the sum rules for the moments do not work at $Q^2 = 0$, where the perturbation series diverges and the G^3 contribution is large. The domain in the (n, Q^2) plane where the sum rules are legitimate is found. A strong correlation of the values of gluon condensate and $\overline{\rm MS}$ charm quark mass is determined. The absolute limits are found to be for the gluon condensate $\langle(\alpha_s/\pi)G^2\rangle = 0.009 \pm 0.007\,\mathrm{GeV}^4$ and for the charm quark mass $\bar{m}(\bar{m}) = 1.275 \pm 0.015\,\mathrm{GeV}$ in the $\overline{\rm MS}$ scheme.

1 Introduction

It is well known that the QCD vacuum generates various quark and gluon condensates, the vacuum expectation values of quark and gluon fields of non-perturbative origin. Among them the gluon condensate $\langle(\alpha_s/\pi)G^a_{\mu\nu}G^a_{\mu\nu}\rangle$, where $G^a_{\mu\nu}$ is the gluon field strength tensor and $\alpha_s = g_s^2/(4\pi)$ is the running QCD coupling constant, plays a special role. The existence of the gluon condensate in QCD was first demonstrated by Shifman, Vainstein and Zakharov [1]. Its special role is caused by a few reasons. First, it has the lowest dimension, $d = 4$, among the gluon condensates as well as any other condensates conserving chirality. For this reason the gluon condensate is the most important one in the determination of the hadronic properties by QCD sum rules, if chirality conserving amplitudes are considered (e.g. in the case of the meson mass determination). Second, the value of the gluon condensate is directly related to the vacuum energy density ε. As was shown in [1],

$$\varepsilon = -\frac{\pi}{8\alpha_s^2}\beta(\alpha_s)\left\langle\frac{\alpha_s}{\pi}G^a_{\mu\nu}G^a_{\mu\nu}\right\rangle, \qquad (1)$$

where $\beta(\alpha_s)$ is the Gell-Mann–Low β-function. Therefore, the sign and magnitude of $\langle(\alpha_s/\pi)G^2\rangle$ are very important for the theoretical description of the QCD vacuum and for the construction of hadron models (e.g. the bag model). Third, in some models the numerical value of the gluon condensate is usually used as a normalization scale which fixes the model parameters. For example, in the instanton model it is required that this value is reproduced by the model.

The numerical value of the gluon condensate

$$\left\langle\frac{\alpha_s}{\pi}G^a_{\mu\nu}G^a_{\mu\nu}\right\rangle = 0.012\,\mathrm{GeV}^4 \qquad (2)$$

has been found in [1] from charmonium sum rules. (This value is often referred to as the standard or SVZ value.) Later there were many attempts to determine the gluon condensate by considering various processes within various approaches. In some of them the value (2) (or ones by a factor of 1.5 higher) was confirmed [2–6], in others it was claimed that the actual value of the gluon condensate is by a factor 2–5 higher than (2) [7–14].

From today's point of view the calculations performed in [1] have a serious drawback. Only the first-order (NLO) perturbative correction was accounted in [1] and there was taken a rather low value of α_s, which was not later confirmed by the experimental data. (It was assumed that the QCD parameter obeys $\Lambda^{(3)} \approx 100\,\mathrm{MeV}$ and $\alpha_s(m_c) \approx 0.2$; today's values are essentially higher.) The contribution of the next, dimension 6, operator G^3 was neglected, so the convergence of the operator product expansion was not tested. In charmonium sum rules the moments $M_n(Q^2)$ of the polarization function $\Pi(q^2)$, $q^2 = -Q^2$ were calculated at the point $Q^2 = 0$. It was shown in [14] that the higher-order terms of the operator product expansion (OPE), namely the contributions of the G^3 and G^4 operators, are of importance at $Q^2 = 0$. The results of calculations of the second-order (NNLO) perturbative corrections to $\Pi(q^2)$ as well as the α_s correction to the gluon con-

[a] e-mail: ioffe@vitep1.itep.ru
[b] e-mail: zyablyuk@heron.itep.ru

densate are available now. They demonstrate that both of them as a rule are large and by no means can be neglected in the sum rules for the moments at $Q^2 = 0$. Finally, the experimental data shifted significantly in comparison with the ones used in [1].

Later the charmonium sum rules were considered at the NLO level in [2] for $Q^2 > 0$, and their analysis basically confirmed the results of [1]. There are recent publications [15–17] where the charmonium as well as bottomonium sum rules were analyzed at $Q^2 = 0$ with α_s^2 perturbative corrections in order to extract the charm and bottom quark masses in the various schemes. The condensate is usually taken to be 0 or some another fixed value. However, the charm mass and the condensate values are entangled in the sum rules. This can easily be understood for large Q^2, where the mass and condensate corrections to the polarization operator behave as some series in negative powers of Q^2, and one may eliminate the condensate contribution to a great extent by slightly changing the quark mass. Vice versa, different condensate values may vary the charm quark mass within a few percents.

The condensate could be also determined from other sum rules, which do not involve the charm quark mass, but the accuracy usually appears to be rather low for this purpose. In particular, a precise analysis of e^+e^- data [18] leads only to rather weak restrictions on the gluon condensate. In [19] a thorough analysis of hadronic τ-decay structure functions was performed and the restriction $\langle(\alpha_s/\pi)G^2\rangle = 0.006 \pm 0.012\,\mathrm{GeV}^4$ was found. This value, however, does not exclude a zero value of the condensate.

For all these reasons a reconsideration of the problem is necessary. The charmonium sum rules on the next level of precision in comparison with [1] is presented below. In Sect. 2 a general outline of the method is given and the experimental input data for the sum rules are presented. In Sect. 3 the method of calculation of the perturbative part of the moments is exposed with the references to the sources we used in the calculations. Section 4 presents the gluon condensate contribution with α_s corrections in a form convenient for numerical evaluation of the moments for non-zero Q^2. In Sect. 5 the perturbative and operator product expansion of the moments is considered. It is argued that the choice of the pole charm quark mass as a mass parameter is not suitable, since in this case the terms of higher order in α_s overwhelm the lower-order ones and the α_s series are divergent. It is proposed to get rid of this problem by using the $\overline{\mathrm{MS}}$ mass as the mass parameter. In what follows the $\overline{\mathrm{MS}}$ charm quark mass $\bar{m}(\bar{m})$ at the renormalization point, equal to the mass itself, is used. The formulae for the moments $\bar{M}_n(Q^2)$, expressed through the $\overline{\mathrm{MS}}$ mass, are given and the domain in the (n, Q^2) plane was found by direct calculation, where the perturbative series are well convergent. In Sect. 6 the calculation of $\bar{m}(\bar{m})$ and of the gluon condensate is presented. In Sect. 7 the sensitivity of the results to the G^3 operator contribution is tested. Section 8 is devoted to a discussion of the attempts to sum up the Coulomb-like corrections. Section 9 contains the conclusions.

2 Experimental current correlator

Consider the two-point correlator of the vector charm currents

$$\mathrm{i}\int \mathrm{d}x \mathrm{e}^{\mathrm{i}qx}\,\langle TJ_\mu(x)J_\nu(0)\rangle = (q_\mu q_\nu - g_{\mu\nu}q^2)\Pi(q^2),$$
$$J_\mu = \bar{c}\gamma_\mu c. \tag{3}$$

The polarization function $\Pi(q^2)$ can be reconstructed by its imaginary part with the help of the dispersion relation

$$R_c(s) = 4\pi\mathrm{Im}\Pi(s+\mathrm{i}0), \quad \Pi(q^2) = \frac{q^2}{4\pi^2}\int_{4m^2}^{\infty}\frac{R_c(s)\mathrm{d}s}{s(s-q^2)}. \tag{4}$$

We shall use the notation R_c, not to be confused with the frequently used notation R for the imaginary part of the electromagnetic current correlator, $R(s) = \sum_f 3Q_f^2 R_f(s)$; we have the normalization $R_c(\infty) = 1$ in the parton model. In the narrow-width approximation $R_c(s)$ can be represented as the sum of the resonance δ-functions:

$$R_c(s) = \frac{3\pi}{Q_c^2\alpha_{\mathrm{em}}^2(s)}\sum_\psi m_\psi \Gamma_{\psi\to ee}\delta(s-m_\psi^2), \tag{5}$$

where $Q_c = 2/3$ is the electric charge of the c quark, and $\alpha_{\mathrm{em}}(s)$ is the running electromagnetic coupling:

$$\alpha_{\mathrm{em}}(s) = \frac{\alpha(0)}{1-\Delta\alpha(s)}, \tag{6}$$
$$\Delta\alpha(s) = -4\pi\alpha(0)\Pi_{\mathrm{em}}(-s) = \Delta\alpha_{\mathrm{lep}}(s) + \Delta\alpha_{\mathrm{had}}(s).$$

Here $\alpha(0) = 1/137.04$ is the fine structure constant, $\Pi_{\mathrm{em}}(s)$ is the correlator of the electromagnetic currents $J_\mu^{\mathrm{em}} = \sum_i Q_i\bar{\psi}_i\gamma_\mu\psi_i$ defined in the same way as (3). As usual, the leptonic contribution to $\Pi_{\mathrm{em}}(s)$ is found by the perturbation theory, while the hadronic contribution has to be determined by a numerical integration of the experimental e^+e^- (or τ-decay) data. Since $\alpha_{\mathrm{em}}(s)$ weakly changes from one resonance to another, we fix it at $s = m_{J/\psi}^2$ from now on:

$$\Delta\alpha_{\mathrm{lep}}(m_{J/\psi}^2) = 0.016, \quad \Delta\alpha_{\mathrm{had}}(m_{J/\psi}^2) = 0.009,$$
$$\alpha_{\mathrm{em}}(m_{J/\psi}^2) = 1/133.6.$$

There are six vector charmonium states with $J^{PC} = 1^{--}$ [20]: see Table 1.

The first two resonances, J/ψ and $\psi(2S)$, are sufficiently narrow and their contribution to $R_c(s)$ can be well parameterized by the δ-functions (5).

But the next resonances, especially the last three ones, are rather wide and the narrow-width approximation for them could be inaccurate. Here it is better to use $R_c(s)$, as extracted from the $e^+e^- \to$ hadrons branching ratio $R(s) = \sum_f 3Q_f^2 R_f(s)$, which is measured experimentally in a wide range of s. Precise data on $R(s)$ in the region of high charmonium states were obtained recently by the BES collaboration [21]. In order to extract $R_c(s)$ from

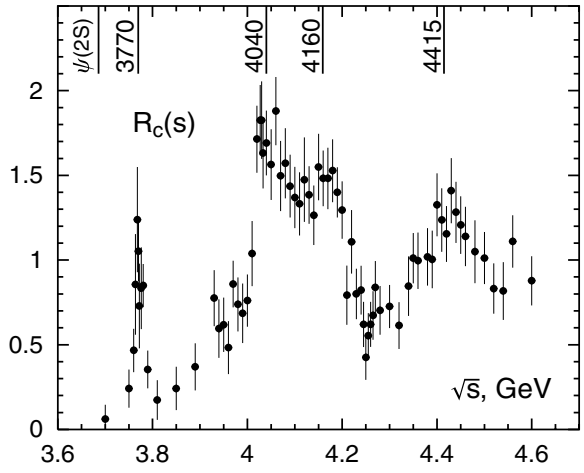

Fig. 1. $R_c(s)$ in the region of high resonances, determined from BES data [21]

Table 1. Six vector charmonium states with $J^{PC} = 1^{--}$

Notation	mass, MeV	full width, MeV	$\Gamma_{\psi\to ee}$, keV
J/ψ(1S)	3096.87 ± 0.04	0.087 ± 0.005	5.26 ± 0.37
ψ(2S)	3685.96 ± 0.09	0.300 ± 0.025	2.19 ± 0.15
$\psi(3770)$	3769.9 ± 2.5	23.6 ± 2.7	0.26 ± 0.04
$\psi(4040)$	4040 ± 10	52 ± 10	0.75 ± 0.15
$\psi(4160)$	4159 ± 20	78 ± 20	0.77 ± 0.23
$\psi(4415)$	4415 ± 6	43 ± 15	0.47 ± 0.10

these data, one has to subtract the contribution of the light quarks from $R(s)$. We suppose that it is well described by the perturbative QCD, which gives 2.16. The result for $R_c(s)$ is shown in Fig. 1. Above the last resonance $R_c(s)$ is getting close to 1, the parton model prediction.

Now we summarize the following experimental input for $R_c(s)$, which will be used in our calculations:

$$\begin{aligned} &s < s_1 = (3.7\,\mathrm{GeV})^2 : && \delta\text{-functions from } J/\psi \text{ and} \\ &&& \psi(2\mathrm{S}) \text{ according to (5)}, \\ &s_1 < s < s_2 = (4.6\,\mathrm{GeV})^2 : && \text{BES data, see Fig. 1}, \\ &s_2 < s : && \text{continuum, } R_c(s) = 1. \end{aligned} \tag{7}$$

One could include the α_s correction in the continuum region, but this will not be essential in what follows.

In order to suppress the contribution of the high energy states, one considers the derivatives of the polarization function in the euclidean region $q^2 = -Q^2 < 0$, the so-called moments:

$$M_n(Q^2) \equiv \frac{4\pi^2}{n!}\left(-\frac{\mathrm{d}}{\mathrm{d}Q^2}\right)^n \Pi(-Q^2) = \int_0^\infty \frac{R_c(s)\mathrm{d}s}{(s+Q^2)^{n+1}}. \tag{8}$$

The experimental values are calculated according to (7):

$$M_n(Q^2) = \frac{27\pi}{4\alpha_{\mathrm{em}}^2}\sum_{\psi=1}^{2}\frac{m_\psi \Gamma_{\psi\to ee}}{(m_\psi^2+Q^2)^{n+1}} + \int_{s_1}^{s_2}\frac{R_c(s)\mathrm{d}s}{(s+Q^2)^{n+1}} + \frac{1}{n(s_2+Q^2)^n}. \tag{9}$$

The squared error of the moments (9) is computed as the sum of the squared errors of each term.

The lowest state J/ψ gives a maximal contribution to the moments due to the largest width $\Gamma_{J/\psi\to ee}$, which itself has the error 7%. This error can be eliminated to a great extent, if one considers the ratio of two moments, which in the general case can be written in the following form:

$$r(n_1,n_2;Q^2) \equiv \frac{M_{n_1}(Q^2)}{M_{n_2}(Q^2)} = (m_{J/\psi}^2+Q^2)^{n_2-n_1}\frac{1+D_1}{1+D_2}, \tag{10}$$

where $D_{1,2}$ denotes the higher state contribution to the moments (9) divided by the J/ψ contribution. Then the error of this ratio is calculated by the usual rules:

$$\left(\frac{\Delta r}{r}\right)^2 = \sum_{j=1}^{2}\left(\frac{\Delta D_j}{1+D_j}\right)^2, \tag{11}$$

where the mass errors are neglected. If $D_{1,2} \ll 1$, the relative error of the ratio is much smaller than the relative errors of the moments itself. This fact has been utilized in many papers on charmonium sum rules and will be used here.

In our calculations we shall always use a sufficiently high n ($n \geq 8$), so that the last term in (9), which comes from the continuum, is small compared to the resonance contribution and the uncertainty introduced by this term is negligible. Moreover, the difference between the narrow-width approximation for the high resonances (above ψ(2S)) as given by (5), and their representation by (7) is small and well below the quoted errors.

3 Theoretical $R(s)$

At first one defines the running QCD coupling $a(\mu^2) \equiv \alpha_s(\mu^2)/\pi$ as a solution of the renormalization group equation:

$$\int_{a(\mu_0^2)}^{a(\mu^2)}\frac{\mathrm{d}a}{\beta(a)} = -\ln\frac{\mu^2}{\mu_0^2}, \quad \beta(a) = \sum_{n\geq 0}\beta_n a^{n+2}. \tag{12}$$

Then the functions $R^{(n)}(s,\mu^2)$ are defined as the coefficients in the α_s expansion:

$$R_c(s) = \sum_{n\geq 0} R^{(n)}(s,\mu^2)a^n(\mu^2). \tag{13}$$

Since $R_c(s)$ is the physical quantity, it does not depend on the scale μ^2, although each term in (13) may be μ^2 dependent.

It is easier to represent the results in terms of the pole quark mass m and the velocity $v = (1-4m^2/s)^{1/2}$. The first two terms in the expansion (13) do not depend on μ^2.

The leading term $R^{(0)}$ was calculated in [22], the next-to-leading $R^{(1)}$ in [23]:

$$\begin{aligned} R^{(0)} &= \frac{v}{2}(3-v^2), \\ R^{(1)} &= \frac{v}{2}(5-3v^2) + 2v(3-v^2)\left(\ln\frac{1-v^2}{4} - \frac{4}{3}\ln v\right) \\ &+ \frac{v^4}{3}\ln\frac{1+v}{1-v} + \frac{4}{3}(3-v^2)(1+v^2) \\ &\times \left[2\mathrm{Li}_2\left(\frac{1-v}{1+v}\right) + \mathrm{Li}_2\left(-\frac{1-v}{1+v}\right)\right. \\ &+ \left.\left(\frac{3}{2}\ln\frac{1+v}{2} - \ln v + \frac{11}{16}\right)\ln\frac{1+v}{1-v}\right], \end{aligned} \tag{14}$$

where $\mathrm{Li}_2(x) = \sum_{n=1}^{\infty} x^n/n^2$ is the dilogarithm function. The function $R^{(2)}$ is usually decomposed into four gauge invariant terms:

$$R^{(2)} = C_F^2 R_{\mathrm{A}}^{(2)} + C_{\mathrm{A}} C_F R_{\mathrm{NA}}^{(2)} + C_F T n_l R_l^{(2)} + C_F T R_F^{(2)}, \tag{15}$$

where $C_{\mathrm{A}} = 3$, $C_F = 4/3$, $T = 1/2$ are group factors, and $n_l = n_f - 1$ is the number of light quarks. The function $R_l^{(2)}$ comes from the diagram with two quark loops: one loop with massive quark, which couples to the vector currents, and another loop with massless quark (the so-called double bubble diagram). It was originally found in [24] and in our normalization takes the form

$$R_l^{(2)} = \left(-\frac{1}{4}\ln\frac{\mu^2}{4s} - \frac{5}{12}\right) R^{(1)} + \delta^{(2)}, \tag{16}$$

where the function $\delta^{(2)}$ is given by (B.3) in [25]. The function $R_F^{(2)}$ comes from the similar double bubble diagram with equal quark masses and has the form [26]

$$R_F^{(2)} = \rho^V + \rho^R - \frac{1}{4}R^{(1)}\ln\frac{\mu^2}{m^2}, \tag{17}$$

where ρ^V is given by (12) in [26]. The function ρ^R comes from the four-particle cut and vanishes for $s < 16m^2$. It is represented as the double integral (13) in [26] which can be computed numerically. However, for $s > 16m^2$ the total function $R_F^{(2)}$ can be well approximated by its high energy asymptotic:

$$R_F^{(2)} = -\frac{1}{4}R^{(1)}\ln\frac{\mu^2}{s} + \zeta_3 - \frac{11}{8} - \frac{13}{2}\frac{m^2}{s} + O\left(m^4/s^2\right). \tag{18}$$

In numerical calculations we take all the terms up to m^{12}/s^6, extracted from [27]. The functions $R_{\mathrm{A}}^{(2)}$ and $R_{\mathrm{NA}}^{(2)}$ are generated by the diagrams with a single quark loop and various gluon exchanges, $R_A^{(2)}$ is an abelian part while $R_{\mathrm{NA}}^{(2)}$ contains purely non-abelian contributions. They are not known analytically. We will use the approximations, given by (65) and (66) in [25] (divided by 3 in our conventions) which reproduce all known asymptotics and Pade approximations with a high accuracy.

4 Condensate contribution

The contribution of the dimension 4 gluon condensate $\langle aG^2\rangle \equiv \langle(\alpha_{\mathrm{s}}/\pi)G^a_{\mu\nu}G^a_{\mu\nu}\rangle$ to the polarization function of massive quarks has the form

$$\Pi^{(G)}(-Q^2) = \frac{\langle aG^2\rangle}{(4m^2)^2}\left[f^{(0)}(z) + af^{(1)}(z)\right],$$

where

$$z = \frac{-Q^2}{4m^2},$$

The leading-order function was found in [1]:

$$f^{(0)}(z) = -\frac{1}{12z^4v^4}\left[\frac{3}{8}\frac{2z-1}{zv}\ln\frac{v-1}{v+1} + z^2 - z + \frac{3}{4}\right], \tag{19}$$

where $v = (1-1/z)^{1/2}$. For this function the following dispersion-like relation can be written:

$$f^{(0)}(z) = -\frac{1}{12}\int_1^{\infty}\frac{\mathrm{d}z'}{z'^3v'}\left[\frac{3}{4}\frac{1}{(z'-z)^2} + \frac{z'}{(z'-z)^3}\right]. \tag{20}$$

This representation is convenient for an evaluation of the various transformations of the polarization function $\Pi(s)$, in particular, the moments.

The next-to-leading order function $f^{(1)}$ was explicitly found in [12]. One could differentiate it n times to obtain the moments for arbitrary Q^2. However, we prefer to construct the dispersion integral similar to (20). The function $f^{(1)}(z)$ has a cut from $z = 1$ to ∞ and behaves as v^{-6} at $z \to 1$. Integrating $f^{(1)}(z')/(z'-z)$ by z' along the contour around the cut, one obtains the following representation:

$$\begin{aligned} f^{(1)}(z) &= \frac{1}{\pi}\int_{1+\epsilon}^{\infty}\frac{\mathrm{Im}f^{(1)}(z'+\mathrm{i}0)}{z'-z}\mathrm{d}z' + \sum_{i=1}^{3}\frac{\pi^2 f_i}{(1-z)^i} \\ &- \frac{65}{1152}\frac{\epsilon^{-3/2}}{1-z} + \left[\frac{8633}{6912} + \frac{17}{36}\ln(8\epsilon)\right]\frac{\epsilon^{-1/2}}{1-z} \\ &+ \frac{65}{384}\frac{\epsilon^{-1/2}}{(1-z)^2}, \end{aligned} \tag{21}$$

where $\epsilon \to 0$ and

$$f_1 = -\frac{17}{384}, \quad f_2 = -\frac{413}{6912}, \quad f_3 = -\frac{197}{2304}. \tag{22}$$

The imaginary part is

$$\begin{aligned} \mathrm{Im}f^{(1)}(z+\mathrm{i}0) &= \frac{\pi}{96z^5v^5}\left[P_2^V(z) + \frac{P_3^V(z)}{zv}\ln\frac{1-v}{1+v}\right. \\ &+ \left.P_4^V(z)(1-z)\left(2\ln v + \frac{3}{2}\ln(4z)\right)\right], \end{aligned} \tag{23}$$

where the polynomials $P_i^V(z)$ are given in Table 1 of [12]. It behaves as v^{-5} at $z \to 1$, so the integral in (21) is

divergent in the limit $\epsilon \to 0$. We decompose it into three parts:

$$\frac{1}{\pi}\mathrm{Im} f^{(1)}(z+\mathrm{i}0) = F_1(z) + F_2'(z) + \frac{1}{2}F_3''(z), \qquad (24)$$

in such way that each function $F_i(z)$ behaves as v^{-1} at $z \to 1$ and has the appropriate asymptotic at $z \to \infty$. In particular we choose

$$\begin{aligned}
F_1(z) &= \frac{1}{96z^4 v}\left[\frac{1627}{36} + \frac{893}{9}z - \frac{98}{3}z^2 + 368z^3\right.\\
&+ \left(\frac{89}{6} - 22z - \frac{140}{3}z^2\right.\\
&+ \left.\left.\frac{3208}{3}z^3 - 3232z^4 + 2208z^5\right)\frac{1}{zv}\ln\frac{1-v}{1+v}\\
&+ \left(68z + \frac{1688}{9}z^2 - \frac{4256}{3}z^3 + 1472z^4\right)\\
&\times \left.\left(2\ln v + \frac{3}{2}\ln(4z)\right)\right],\\
F_2(z) &= \frac{1}{96z^4 v}\left[-\frac{23}{4} + \frac{559}{18}z + \frac{272}{3}z^2\right.\\
&+ \left(-\frac{197}{8} + \frac{947}{72}z\right)\frac{1}{zv}\ln\frac{1-v}{1+v}\\
&+ \left.\frac{136}{3}z^2\left(2\ln v + \frac{3}{2}\ln(4z)\right)\right],\\
F_3(z) &= \frac{1}{96z^3 v}\left[-\frac{67}{6} - \frac{197}{12zv}\ln\frac{1-v}{1+v}\right]. \qquad (25)
\end{aligned}$$

Then one may integrate (21) by parts twice and all terms singular in ϵ cancel. Eventually we obtain the following representation for the function $f^{(1)}$:

$$f^{(1)}(z) = \sum_{i=1}^{3}\left[\frac{\pi^2 f_i}{(1-z)^i} + \int_1^\infty \frac{F_i(z')}{(z'-z)^i}\mathrm{d}z'\right]. \qquad (26)$$

It will be used to compute the moments numerically.

5 Moments in the $\overline{\mathrm{MS}}$ scheme

For definiteness let us choose the scale $\mu^2 = m^2$ in (13) and write down the α_s expansion of the moments (8):

$$\begin{aligned}
M_n(Q^2) &= \sum_{k\geq 0} M_n^{(k)}(Q^2)a^k(m^2)\\
&+ \left\langle\frac{\alpha_\mathrm{s}}{\pi}G^2\right\rangle\sum_{k\geq 0} M_n^{(G,k)}(Q^2)a^k(m^2). \qquad (27)
\end{aligned}$$

The perturbative coefficient functions are

$$M_n^{(k)}(Q^2) = \int_{4m^2}^\infty \frac{R_n^{(k)}(s,m^2)\mathrm{d}s}{(s+Q^2)^{n+1}}. \qquad (28)$$

The leading order can be expressed via the Gauss hypergeometric function:

$$\begin{aligned}
M_n^{(0)}(Q^2) &= \frac{1}{(4m^2)^n}\frac{3\sqrt{\pi}}{4}\frac{(n+1)\Gamma(n)}{\Gamma(n+5/2)}\\
&\times {}_2F_1\left(\left.\begin{matrix}n, n+2\\ n+5/2\end{matrix}\right| -\frac{Q^2}{4m^2}\right). \qquad (29)
\end{aligned}$$

The higher-order functions $M^{(1)}$ and $M^{(2)}$ are computed numerically by (28). (Notice that the analytical expression for $M_n^{(1)}(0)$ has been found in [15] and the first seven moments $M_n^{(2)}(0)$ can be determined from the low energy expansion of the polarization function $\Pi(s)$ available in [25].)

The leading-order contribution of the gluon condensate is easily obtained from (20):

$$\begin{aligned}
M_n^{(G,0)}(Q^2) &= -\frac{\pi^2}{(4m^2)^{n+2}}\frac{\sqrt{\pi}}{6}\frac{(n+1)\Gamma(n+4)}{\Gamma(n+7/2)}\\
&\times {}_2F_1\left(\left.\begin{matrix}n+2, n+4\\ n+7/2\end{matrix}\right| -\frac{Q^2}{4m^2}\right). \qquad (30)
\end{aligned}$$

The next-to-leading condensate correction can be computed numerically with the help of the integral representation, obtained from (26):

$$\begin{aligned}
M_n^{(G,1)}(Q^2) &= \frac{4\pi^2}{(4m^2)^{n+2}} \qquad (31)\\
&\times \sum_{i=1}^{3}\frac{\Gamma(n+i)}{\Gamma(n+1)\Gamma(i)}\left[\frac{\pi^2 f_i}{(1+y)^{n+i}} + \int_1^\infty \frac{F_i(z)}{(z+y)^{n+i}}\mathrm{d}z\right],
\end{aligned}$$

where $y = Q^2/(4m^2)$, and the constants f_i and the functions $F_i(z)$ are given in (22) and (25).

The pole quark mass m is the most natural choice, since it is the physical invariant. However in the pole scheme the perturbative corrections to the moments are huge. For instance, at the typical point, which will be used later in our analysis, one gets

$$\begin{aligned}
n = 10, Q^2 = 4m^2: \ &\frac{M^{(1)}}{M^{(0)}} = 13.836, \qquad (32)\\
&\frac{M^{(2)}}{M^{(0)}} = 193.33, \quad \frac{M^{(G,1)}}{M^{(G,0)}} = 13.791.
\end{aligned}$$

Since in the domain of interest $a \sim 0.1$, this is an indication that the series (27) is divergent. The situation is even worse for $Q^2 = 0$ (see [15]). It is almost impossible to choose an informative region in the (n, Q^2) plane where the perturbative corrections in the pole mass scheme are tolerable and the continuum as well as the $\langle G^3\rangle$ contributions are suppressed enough on the other hand.

The traditional solution to this problem is the mass redefinition. In particular, in the most popular $\overline{\mathrm{MS}}$ scheme the mass corrections are known to be significantly smaller. In $\overline{\mathrm{MS}}$ conventions the mass $\bar{m}$ depends on the scale μ^2 according to the RG equation:

$$\bar{m}(\mu^2) = \bar{m}(\mu_0^2)\exp\left(\int_{a(\mu_0^2)}^{a(\mu^2)}\frac{\gamma_m(a)}{\beta(a)}\mathrm{d}a\right),$$

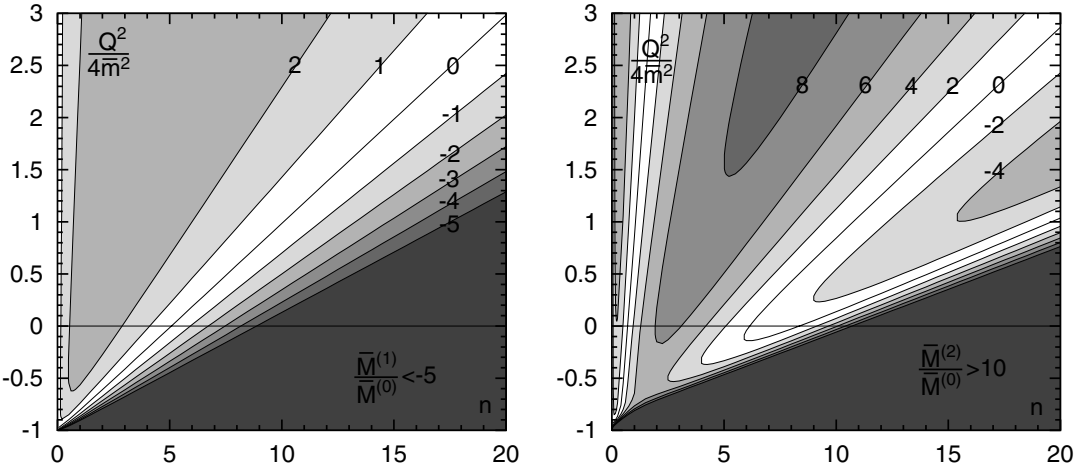

Fig. 2. Ratio $\bar{M}_n^{(1)}/\bar{M}_n^{(0)}$ (*left*) and $\bar{M}_n^{(2)}/\bar{M}_n^{(0)}$ (*right*) in the $(n,\, Q^2)$ plane

$$\gamma_m(a) = \sum_{n\geq 0} \gamma_n a^{n+1}, \tag{33}$$

where γ_m is the mass anomalous dimension. In what follows we shall choose the most natural mass scale $\mu^2 = \bar{m}^2$ and will denote $\bar{m}(\bar{m}^2)$ simply by $\bar{m}$.

There is a perturbative relation between the pole mass m and the $\overline{\rm MS}$ one $\bar{m}$:

$$\frac{m^2}{\bar{m}^2} = 1 + \sum_{n\geq 1} K_n a^n(\bar{m}^2). \tag{34}$$

The two-loop factor was found, in particular, in [28], while the three-loop factor was recently calculated in [29]:

$$\begin{aligned} K_1 &= \frac{8}{3}, \\ K_2 &= 28.6646 - 2.0828 n_l = 22.4162, \\ K_3 &= 417.039 - 56.0871 n_l + 1.3054 n_l^2 = 260.526. \end{aligned} \tag{35}$$

We put $n_l = 3$ in the last column. The series (34) also looks divergent at the charm scale. (Notice, that the authors of [1] used another mass convention, although numerically close to $\overline{\rm MS}$ scheme at the NLO level: the coefficient K_1 was equal to $4\ln 2$ there.)

Nevertheless let us assume for a moment that $\alpha_{\rm s}$ is small; take advantage of (34) and (35) and express the moments (8) in terms of the mass $\bar{m}$:

$$\begin{aligned} M_n(Q^2) = &\sum_{k\geq 0} \bar{M}_n^{(k)}(Q^2) a^k(\bar{m}^2) \\ &+ \left\langle \frac{\alpha_{\rm s}}{\pi} G^2 \right\rangle \sum_{k\geq 0} \bar{M}_n^{(G,k)}(Q^2) a^k(\bar{m}^2). \end{aligned} \tag{36}$$

As follows from the definition (8) and the dimensional consideration

$$\begin{aligned} \bar{M}_n^{(0)}(Q^2) &= M_n^{(0)}, \\ \bar{M}_n^{(1)}(Q^2) &= M_n^{(1)} - K_1(n-d/2) M_n^{(0)} \\ &\quad + K_1(n+1) Q^2 M_{n+1}^{(0)}, \\ \bar{M}_n^{(2)}(Q^2) &= M_n^{(2)} - K_1(n-d/2) M_n^{(1)} \\ &\quad + K_1(n+1) Q^2 M_{n+1}^{(1)} \\ &\quad + (n-d/2)\left[\frac{K_1^2}{2}(n+1-d/2) - K_2\right] M_n^{(0)} \\ &\quad + (n+1)\left[K_2 - K_1^2(n+1-d/2)\right] Q^2 M_{n+1}^{(0)} \\ &\quad + \frac{K_1^2}{2}(n+1)(n+2) Q^4 M_{n+2}^{(0)}, \\ \bar{M}_n^{(G,0)}(Q^2) &= M_n^{(G,0)}, \\ \bar{M}_n^{(G,1)}(Q^2) &= M_n^{(G,1)} - K_1(n+2-d/2) M_n^{(G,0)} \\ &\quad + K_1(n+1) Q^2 M_{n+1}^{(G,0)}, \end{aligned} \tag{37}$$

where d is the dimension of the polarization function $\Pi(Q^2)$ ($d = 0$ for vector currents). All $M_n^{(i)}$ in the r.h.s. are computed with the $\overline{\rm MS}$ mass $\bar{m}$.

The moment corrections $\bar{M}^{(k)}$ are much smaller than $M^{(k)}$ in the pole scheme. In particular, at the same point, which was considered in (32), we have now

$$\begin{aligned} n = 10, Q^2 = 4\bar{m}^2: \quad &\frac{\bar{M}^{(1)}}{\bar{M}^{(0)}} = 0.045, \quad \frac{\bar{M}^{(2)}}{\bar{M}^{(0)}} = 1.136, \\ &\frac{\bar{M}^{(G,1)}}{\bar{M}^{(G,0)}} = -1.673. \end{aligned} \tag{38}$$

This smallness of the corrections as compared to the pole scheme is observed for almost all n and Q^2. The ratios $\bar{M}_n^{(1)}/\bar{M}_n^{(0)}$ and $\bar{M}_n^{(2)}/\bar{M}_n^{(0)}$ are shown in Fig. 2 and the ratio $\bar{M}_n^{(G,1)}/\bar{M}_n^{(G,0)}$ in Fig. 3 for $n = 0\ldots 20$ and $Q^2/(4\bar{m}^2) = -1\ldots 3$. The perturbative expansion in the $\overline{\rm MS}$ scheme obviously does not work in the area of high n and low Q^2, marked with dark. (The detailed data are presented in Tables 2,3,4 in the appendix.)

Now we can argue why the expression (37) for the moments is legitimate, despite the series (34), relating the pole mass m and $\overline{\rm MS}$ mass $\bar{m}$, being divergent at the coupling $\alpha_{\rm s}$ taken on the charm mass scale. If $\alpha_{\rm s}$ is small enough, (37) is correct. In this case the same values of $\bar{M}_n$ can be obtained by the procedure, when the

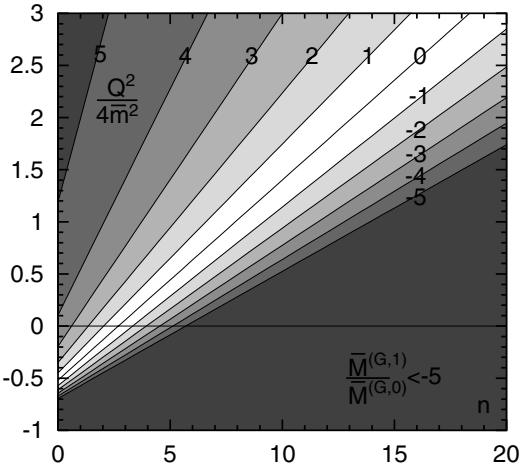

Fig. 3. Ratio $\bar{M}_n^{(G,1)}/\bar{M}_n^{(G,0)}$ in the $(n,\, Q^2)$ plane

$\overline{\rm MS}$ mass renormalization is performed directly in the diagrams, wholly without the concept of the pole mass. If the pole mass concept is not used, the relations (34) and (35) are irrelevant. These relations demonstrate only that the pole mass is an ill defined object in the case of charm. The check of self-consistency of the moments $M_n^{(k)}$ is the convergence of the series (36).

If one takes the QCD coupling at some other scale $\alpha_{\rm s}(\mu^2)$, the function $M^{(2)}$ must be replaced by

$$a(\bar{m}^2) \to a(\mu^2), \qquad (39)$$
$$\bar{M}_n^{(2)}(Q^2) \to \bar{M}_n^{(2)}(Q^2) + \bar{M}_n^{(1)}(Q^2)\beta_0 \ln\frac{\mu^2}{\bar{m}^2},$$

so that the series (36) is μ^2-independent at the order $\alpha_{\rm s}^2$.

6 Determination of the charm quark mass and the gluon condensate from the data

The theoretical moments depend on three parameters: charm quark mass, QCD coupling constant and gluon condensate. The QCD coupling $\alpha_{\rm s}$ is a universal quantity and can be taken from other experiments. In particular, as a boundary condition in the RG equation (12) we put

$$\alpha_{\rm s}(m_\tau^2) = 0.330 \pm 0.025, \quad m_\tau = 1.777\,{\rm GeV}, \qquad (40)$$

found from hadronic τ-decay analysis [19] at the τ mass in agreement with other data [20].

Another question is the choice of the scale μ^2, at which $\alpha_{\rm s}$ should be taken. Since the higher-order perturbative corrections are not known, the moments $M_n(Q^2)$ will depend on this scale. In the massless limit the most natural choice is $\mu^2 = Q^2$. On the other hand for massive quarks and $Q^2 = 0$ the scale is usually taken $\mu^2 \sim m^2$. So we choose the interpolation formula

$$\mu^2 = Q^2 + \bar{m}^2. \qquad (41)$$

At this scale $\alpha_{\rm s}$ is smaller than at $\mu^2 = \bar{m}^2$ for the price of a larger $\bar{M}_n^{(2)}$ according to (39). (Notice that in the tables in the appendix as well as in Fig. 2 the ratio $\bar{M}^{(2)}/\bar{M}^{(0)}$ is given at the scale $\mu^2 = \bar{m}^2$.) Sometimes we will vary the coefficient before $\bar{m}^2$ of (41) to test the dependence of the results on the scale.

The sum rules for the low-order moments $M_n(Q^2)$, $n \le 3$, cannot be used because of the large contribution of the high excited states and continuum as well as the large $\alpha_{\rm s}^2$ corrections (see the tables in the appendix), especially at $Q^2 = 0$. As Fig. 3 demonstrates, at $n \ge 4$ the $\alpha_{\rm s}$ correction to the gluon condensate is large at $Q^2 = 0$. The $\langle G^3\rangle$ condensate contribution is also large (see below), which demonstrates that the operator product expansion is divergent here. For these reasons we will avoid using the sum rules at small Q^2.

As Fig. 2 shows, the first correction to the moments $\bar{M}_n^{(1)}(Q^2)$ vanishes along the diagonal line, approximately parameterized by the equation $Q^2/(4\bar{m}^2) = n/5 - 1$. The second-order correction $\bar{M}^{(2)}$ and the correction to the condensate contribution $\bar{M}^{(G,1)}$ are also small along this diagonal for $n > 5$. Now let us compare the theoretical moments with the experimental value (9) at different points on this diagonal. If the condensate is fixed, then one can numerically solve this equation in order to find the $\overline{\rm MS}$ mass. The result is shown in Fig. 4a. The values $n < 5$ are not reliable, since the $\alpha_{\rm s}$ correction to the condensate exceeds -50% here.

The lines in Fig. 4a are almost horizontal if the condensate is not too large. Consequently there is a correlation between the mass and condensate and we establish the dependence of the $\overline{\rm MS}$ charm mass $\bar{m}$ on the condensate $\langle(\alpha_{\rm s}/\pi)G^2\rangle$ found at the point $n = 10$, $Q^2 = 0.98 \times 4\bar{m}^2$ on this diagonal. It is plotted in Fig. 4b. The error of the experimental moments is about 7%, arising mainly from the uncertainty in $\Gamma_{J/\psi\to ee}$. But, since $M_n(Q^2) \sim (4\bar{m}^2 + Q^2)^{-n}$, the mass error is of order $7/n\%$, i.e. is much smaller. For instance, at zero condensate

$$\bar{m}(\bar{m}^2) = 1.283 \pm 0.007\,{\rm GeV} \quad \text{for} \quad \left\langle \frac{\alpha_{\rm s}}{\pi} G^2 \right\rangle = 0; \quad (42)$$

the error is purely experimental. The dependence plotted in Fig. 4b as well as the value (42) are weakly sensitive to the particular choice of the QCD coupling $\alpha_{\rm s}$ and the scale μ^2. This is an obvious advantage of the non-zero Q^2, while the analysis at $Q^2 = 0$ leads to a significantly higher error [17].

It is more difficult to find the restrictions on the mass and condensate separately. For this purpose one has to choose the point in the (n, Q^2) plane which is

(1) out of the diagonal, since no new information can be obtained from there,
(2) not in the lower right corner (high n, low Q^2), where perturbative corrections as well as $\alpha_{\rm s}$ corrections to the gluon condensate are large, and
(3) not in the upper left corner (low n, high Q^2), where the continuum contribution to the experimental moments is uncontrollable. It turns out that if one considers the ratio of the moments (10), the mass–condensate dependence appears to be different in comparison to Fig. 4b. In particular, the results obtained from the ratio M_{10}/M_{12} at

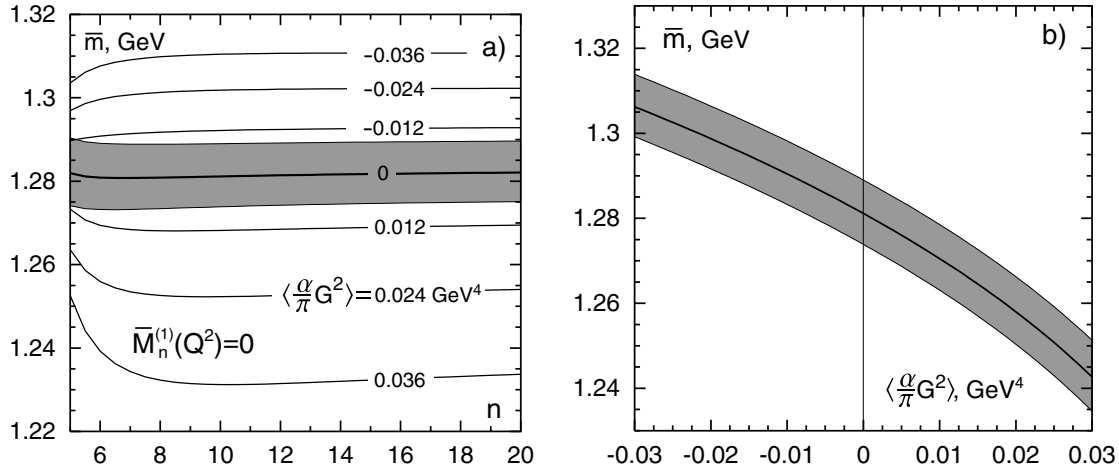

Fig. 4. **a** $\overline{\rm MS}$ mass found from the experimental moments $M_n(Q_n^2)$ for different n and Q_n^2 determined by the equation $\bar{M}_n^{(1)}(Q_n^2)=0$ for different values of the gluon condensate. The shaded area shows the experimental error for $\langle(\alpha_{\rm s}/\pi)G^2\rangle=0$; for non-zero condensates only the central lines are shown. **b** $\bar{m}(\bar{m}^2)$ in GeV versus $\langle(\alpha_{\rm s}/\pi)G^2\rangle$ in GeV^4 determined from $n=10$ and $Q^2=0.98\times 4\bar{m}^2$. $\alpha_{\rm s}$ is taken at the scale (41)

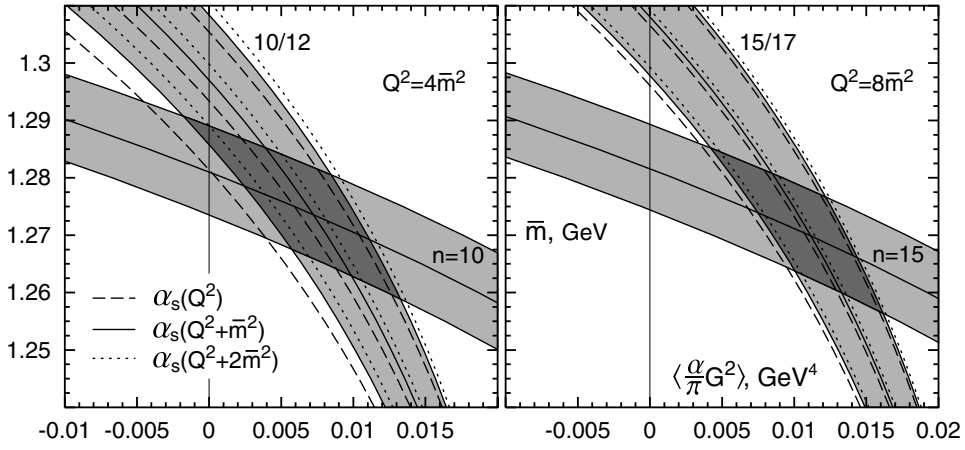

Fig. 5. $\overline{\rm MS}$ mass versus gluon condensate obtained from different points on the (n,Q^2) plane. "Horizontal" bands are obtained from the moments $(10,4\bar{m}^2)$ and $(15,8\bar{m}^2)$, "vertical" bands obtained from the ratio of the moments M_{10}/M_{12} (left), M_{15}/M_{17} (right) for a few different choices of $\alpha_{\rm s}(\mu^2)$

$Q^2=4\bar{m}^2$ and M_{15}/M_{17} at $Q^2=8\bar{m}^2$ are demonstrated in the left and right parts of Fig. 5 respectively. In the same figures the mass-condensate dependence, obtained from the moments $M_{10}(Q^2=4\bar{m}^2)$ and $M_{15}(Q^2=8\bar{m}^2)$, is also plotted. The error bands include both the experimental error of the ratio (11) and the uncertainty of $\alpha_{\rm s}$ (40). Obviously the results, obtained outside the diagonal, are sensitive to the choice of $\alpha_{\rm s}$ as well as μ^2. The small variation of μ^2 slightly changes the acceptable region in Fig. 5, but if one takes μ^2 a few times lower, the region expands to the left significantly.

The absolute limits of the $\overline{\rm MS}$ charm quark mass and the gluon condensate can be determined from Fig. 5:

$$\bar{m}(\bar{m}^2)=1.275\pm0.015\,{\rm GeV},$$
$$\left\langle\frac{\alpha_{\rm s}}{\pi}G^2\right\rangle=0.009\pm0.007\,{\rm GeV}^4. \qquad (43)$$

The restrictions on $\bar{m}$ and the gluon condensate obtained from other ratios of the moments agree with (43), but are weaker (see Fig. 6, where the ratio M_8/M_{10} is considered). The stability intervals in the moments, i.e. the intervals where (43) occurs within the errors were found to be $n=$ 8–13 at $Q^2=4\bar{m}^2$ and $n=12$–19 at $Q^2=8\bar{m}^2$.

As a check, the calculations were performed where the $\alpha_{\rm s}^2$ terms in the $\overline{\rm MS}$ moments were omitted as well as the $\alpha_{\rm s}$ corrections to the gluon condensate contribution ($\bar{M}_n^{(2)}=\bar{M}_n^{(G,1)}=0$). At $Q^2=4\bar{m}^2$ it was found that $\bar{m}=1.266\,{\rm GeV}$ and $\langle aG^2\rangle=0.011\,{\rm GeV}^4$ from M_{10} and M_{10}/M_{12}, while at $Q^2=8\bar{m}^2$ the result $\bar{m}=1.263\,{\rm GeV}$ and $\langle aG^2\rangle=0.015\,{\rm GeV}^4$ was obtained from M_{15} and M_{15}/M_{17}. These values agree with (43) in the limit of the errors. However, it is difficult to estimate the errors of the calculation, where the $\alpha_{\rm s}^2$ terms are omitted because of the uncertainty in the scale.

$R_c(s)$ in (13), or the expression for the moments, are in principle independent on the normalization scale μ^2. However, in fact, since we take into account only the first

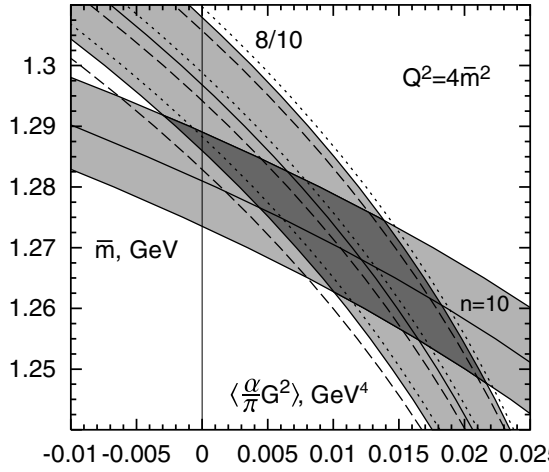

Fig. 6. $\overline{\rm MS}$ mass versus gluon condensate obtained from the ratio M_8/M_{10} above the diagonal. For more on the notation see Fig. 5

three terms in the $\alpha_{\rm s}$ expansion in (27), such a dependence occurs. Namely, when we change the normalization point in $\alpha_{\rm s}$ from $\bar m^2$ to $\mu^2 = Q^2 + \bar m^2$, see (41), with the help of (39), the values of the moments defined by (27) are changed. As is clear from (39), the difference between the moments $M_n(Q^2)$ at the normalization points $\bar m^2$ and $Q^2 + \bar m^2$ increases with Q^2. At Q^2 as used above, the difference is moderate and, if recalculated to $\langle(\alpha_{\rm s}/\pi)G^2\rangle$, results in an error $\Delta\langle(\alpha_{\rm s}/\pi)G^2\rangle \sim 2\times10^{-3}\,{\rm GeV}^4$, much smaller than the overall error in (43). However, going to the higher Q^2 would be dangerous. In fact, while deriving (39), we expanded the running QCD coupling $a(\mu^2)$ in $a(\bar m^2)$. This expansion is valid if

$$a\beta_0 \ln\frac{Q^2}{\bar m^2} \ll 1. \tag{44}$$

In particular for $Q^2/(4\bar m^2) = 3$ the l.h.s. of this equation is ~ 0.5 and the neglected higher-order terms could be significant. For this reason we avoid to use a higher Q^2 than was taken.

Let us now turn the problem around and try to predict the width $\Gamma_{J/\psi\to ee}$ theoretically. In order to avoid the wrong circle argumentation we do not use the condensate value just obtained, but take the limitation $\langle(\alpha_{\rm s}/\pi)G^2\rangle = 0.006 \pm 0.012\,{\rm GeV}^4$ found in [19] from the τ-decay data. Then the mass limits $\bar m = 1.28$–$1.33\,{\rm GeV}$ can be found from the moment ratios exhibited above, which do not depend on $\Gamma_{J/\psi\to ee}$ if the contributions of the higher resonances is approximated by a continuum (the accuracy of such an approximation is about 3%). The substitution of these values of $\bar m$ into the moments gives

$$\Gamma^{\rm theor}_{J/\psi\to ee} = 4.9 \pm 0.8\,{\rm keV}, \tag{45}$$

to be compared with the experimental value $\Gamma_{J/\psi\to ee} = 5.26 \pm 0.37\,{\rm keV}$. Such a good coincidence of the theoretical prediction and experimental data is a very impressive demonstration of the effectiveness of the QCD sum rules.

It must be stressed that while obtaining (45) no additional input was used besides the condensate restriction taken from [19] and the value of $\alpha_{\rm s}(m_\tau^2)$.

7 Influence of the $D = 6$ condensate

The $D = 4$ gluon condensate $\langle aG^2\rangle$ is the leading term in the operator expansion series. The question arises how the higher dimension condensate could change the results of our analysis. There is a single $D = 6$ gluon condensate $\langle g^3G^3\rangle$. Its contribution to the polarization function (3) can be parameterized as follows:

$$\Pi^{(G3)}(s) = \frac{\left\langle g^3 f^{abc} G^a_{\mu\nu} G^b_{\nu\lambda} G^c_{\lambda\mu}\right\rangle}{(4m^2)^3} f^{(G3)}(z), \quad z = \frac{s}{4m^2}.$$

The dimensionless function $f^{(G3)}(z)$ has been found in [30]:

$$f^{(G3)}(z) = -\frac{1}{72\pi^2 z^3} \times \left(\frac{2}{15} + \frac{2}{5}z + 4J_2 - \frac{31}{3}J_3 + \frac{43}{5}J_4 - \frac{12}{5}J_5\right), \tag{46}$$

where the integrals

$$J_n = \int_0^1 \frac{{\rm d}x}{[1 - 4zx(1-x)]^n}$$

can be calculated analytically. However, the integral representation is convenient to express the result in terms of Gauss hypergeometric function, which can be easily differentiated in order to obtain the moments:

$$M_n(Q^2) = M_n^{(0)}(Q^2) + \ldots + \left\langle g^3 f^{abc} G^a_{\mu\nu} G^b_{\nu\lambda} G^c_{\lambda\mu}\right\rangle M_n^{(G3)}(Q^2), \tag{47}$$

where

$$M_n^{(G3)}(Q^2) = \frac{\sqrt{\pi}}{1080(4m^2)^{n+3}} \sum_{i=2}^{4} c_i \frac{\Gamma(n+i)\Gamma(n+5)}{\Gamma(n+1)\Gamma(n+9/2)} \times {}_2F_1\left(\begin{matrix} n+i, n+5 \\ n+9/2 \end{matrix}\middle| -\frac{Q^2}{4m^2}\right)$$

and we have the constants $c_2 = 3$, $c_3 = -7$, $c_4 = -9$. The significance of the condensate $\langle g^3G^3\rangle$ is determined by the ratio of the two terms in (47). The numerical values of this ratio for different (n, Q^2) are given in the last column of Tables 2–4 in the appendix.

No reliable estimations of the $\langle G^3\rangle$ condensate are available. There exists only the estimation based on the dilute instanton gas model [31]:

$$\left\langle g^3 f^{abc} G^a_{\mu\nu} G^b_{\nu\lambda} G^c_{\lambda\mu}\right\rangle = \frac{4}{5}\frac{12\pi^2}{\rho_c^2}\left\langle\frac{\alpha_{\rm s}}{\pi}G^2\right\rangle, \tag{48}$$

where ρ_c is the effective instanton radius. The numerical value of ρ_c is uncertain, even in the framework of the

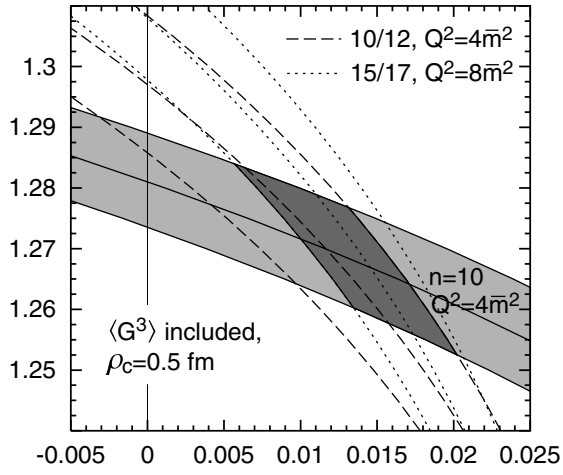

Fig. 7. $\overline{\rm MS}$ mass versus gluon condensate obtained from the moments and ratios with account of the $\langle G^3\rangle$ condensate according to (48)

model: in [32] the value $\rho_c = 1/3\,\text{fm} = 1.5\,\text{GeV}^{-1}$ was advocated, in [1] the value $\rho_c = 1\,\text{fm} = 4.5\,\text{GeV}^{-1}$ was used. In the recent paper [33], based on the sum rules sensitive to the gluon condensate, $\rho_c = 0.5\,\text{fm} = 2.5\,\text{GeV}^{-1}$ was suggested.

The contribution of $\langle g^3G^3\rangle$ to $M_n(Q^2)$ at a fixed n falls rapidly with the growth of Q^2. At $Q^2 = 0$ and $n \geq 5$ it comprises about 50% or more of the gluon condensate contribution at $\rho_c = 0.5\,\text{fm}$. Even at $Q^2/(4\bar{m}^2) = 1$ it is significant: the (negative) correction to the gluon condensate term is $\sim 10\%$ in M_{10} and $\sim 30\%$ in the ratio M_{10}/M_{12}. One gets more reliable results at $Q^2/(4\bar{m}^2) = 2$. Here the corrections are -7% for M_{15} and -18% for M_{15}/M_{17}. These corrections leave the charm quark mass almost unchanged, but increase the gluon condensate and its error (compare Figs. 5 and 7). The account of the $\langle g^3G^3\rangle$ contribution leads to the following restriction:

$$\left\langle \frac{\alpha_\text{s}}{\pi} G^2 \right\rangle = 0.011 \pm 0.009\,\text{GeV}^4. \qquad (49)$$

Certainly, it relies upon the instanton gas model that gives (48).

8 About the attempts to sum up the Coulomb-like corrections

Sometimes when considering the heavy quarkonia sum rules the Coulomb-like corrections are summed up [15,26, 34–37]. The basic argumentation for such a summation is that at $Q^2 = 0$ and high n only small quark velocities $v \lesssim 1/(n^{1/2})$ are essential and the problem becomes non-relativistic. Thus it is possible to perform the summation with the help of well-known formulae of non-relativistic quantum mechanics for $|\psi(0)|^2$ in case of a Coulomb interaction (see [38]).

This method was not used here for the following reasons:

(1) The basic idea of our approach is to calculate the moments of the polarization operator in QCD by applying the perturbation theory and OPE (l.h.s. of the sum rules) and to compare it with the r.h.s. of the sum rules, represented by the contribution of the charmonium states (mainly by J/ψ). Therefore it is assumed that the theoretical side of the sum rule is dual to the experimental one, i.e. the same domains of the coordinate and momentum spaces are of importance at both sides. But the charmonium states (particularly, J/ψ) are by no means the Coulomb systems. A particular argument in favor of this statement is the ratio $\Gamma_{J/\psi\to ee}/\Gamma_{\psi'\to ee} = 2.4$. If charmonia were a non-relativistic Coulomb system, $\Gamma_{\psi\to ee}$ would be proportional to $|\psi(0)|^2 \sim 1/(n_r+1)^3$, and since ψ' is the first radial excitation with $n_r = 1$, this ratio would be equal to 8 (see also [38]).
(2) The heavy quark–antiquark Coulomb interaction at large distances $r > r_\text{conf} \sim 1\,\text{GeV}^{-1}$ is screened by gluon and light quark–antiquark clouds, resulting in string formation. Therefore the summation of a Coulombic series makes sense only when the Coulomb radius r_Coul is below r_conf. (It must be kept in mind that higher-order terms in a Coulombic series represent the contributions of large distances, $r \gg r_\text{Coul}$.) For charmonia we have

$$r_\text{Coul} \approx \frac{2}{m_c C_F \alpha_\text{s}} \approx 4\,\text{GeV}^{-1}.$$

It is clear, that the necessary condition $R_\text{Coul} < R_\text{conf}$ is badly violated for charmonia. This means that the summation of the Coulomb series in case of charmonium would be a wrong step.
(3) Our analysis is performed at $Q^2/4\bar{m}^2 \geq 1$. At large Q^2 the Coulomb corrections are suppressed in comparison with $Q^2 = 0$. It is easy to estimate the characteristic values of the quark velocities. At large n they are $v \approx ((1+Q^2/4m^2)/n)^{1/2}$. We are working along the diagonals of Fig. 4, well parameterized by the equation $Q^2/4\bar{m}^2 \approx n/5 - 1$. Here the quark velocity $v \sim 1/(5^{1/2}) \approx 0.45$ is not small and not in the non-relativistic domain, where the Coulomb corrections are large and legitimate.

Nevertheless, let us look to the expression of R_c, obtained after summation of the Coulomb corrections in the non-relativistic theory [39]. It reads (to go from QED to QCD one has to replace $\alpha \to C_F\alpha_\text{s}$, $C_F = 4/3$):

$$R_{c,\text{Coul}} = \frac{3}{2}\frac{\pi C_F\alpha_\text{s}}{1-\text{e}^{-x}} = \frac{3}{2}v\left(1 + \frac{x}{2} + \frac{x^2}{12} - \frac{x^4}{720} + \dots\right), \qquad (50)$$

where $x = \pi C_F\alpha_\text{s}/v$. At $v = 0.45$ and $\alpha_\text{s} \approx 0.26$ the first three terms in the expansion (50), accounted in our calculations, reproduce the exact value of $R_{c,\text{Coul}}$ with accuracy 1.6%. Such a deviation leads to the error of the mass $\bar{m}$ of order (1–2) $\times\, 10^{-3}\,\text{GeV}$, which is completely negligible. In order to avoid misunderstanding, it must be mentioned that the value of $R_{c\text{Coul}}$, computed by summing the Coulomb corrections in non-relativistic theory, has not too much in common with the real physical situation. Numerically, at the chosen values of the parameters $R_{c\text{Coul}} \approx 1.8$, while the real value (both experimental and

in perturbative QCD) is about 1.1. The goal of the arguments presented above was to demonstrate that even in the case of a Coulombic system our approach would have a good accuracy of calculation.

At $v = 0.45$ the momentum transfer from quark to antiquark is $\Delta p \sim 1\,\mathrm{GeV}$. (This is the typical domain for the QCD sum rule validity.) In coordinate space it corresponds to $\Delta r_{q\bar{q}} \sim 1\,\mathrm{GeV}^{-1}$. Comparison with potential models [39] demonstrates that in this region the effective potential strongly differs from the Coulombic one.

(4) A large compensation of various terms in the expression for the moments in the $\overline{\mathrm{MS}}$ scheme (see Fig. 2) is not achieved if only the Coulomb terms are taken into account. This means that the terms of non-Coulombic origin are more important here than the Coulombic ones.

For all these reasons we believe that the summation of non-relativistic Coulomb corrections is inadequate in the problem considered: it will not improve the accuracy of the calculations, but it would be misleading.

9 Results and discussion

The analysis of charmonium sum rules is performed within the framework of QCD at the next level of precision in comparison with the famous treatment of this problem by Shifman, Vainstein and Zakharov [1]. In the perturbation theory the terms of order α_s^2 were accounted as well as α_s corrections to the gluon condensate contribution, in OPE the dimension 6 operator G^3. The method of the moments was exploited. The validity of the method was demonstrated for the $\overline{\mathrm{MS}}$ mass of the charm quark, but not for the pole mass. The domain in the (n, Q^2) plane was found where the three accounted terms in the perturbative series are well converging. It was shown that the sum rules do not work at $Q^2 = 0$, where the following four requirements cannot be satisfied simultaneously:

(1) convergence of the perturbation series,
(2) a small α_s correction to the gluon condensate contribution,
(3) a small contribution of the G^3 operator,
(4) a small contribution of the higher resonances and continuum.

A large Q^2 allows us also to suppress the Coulomb corrections. The most suitable values of Q^2 for the sum rules are $Q^2 \sim$ (1–2)$4\bar{m}^2 \sim$ 5–15 GeV^2. The values of the charmed quark of $\overline{\mathrm{MS}}$ and the gluon condensate were found by comparing the theoretical moments with the experimental ones, saturated by charmonium resonances (plus continuum). A strong correlation of the values $\bar{m}$ and $\langle(\alpha_s/\pi)G^2\rangle$ was established. This connection only weakly depends on α_s. Taking the α_s value found in [19] from the hadronic τ-decay data,

$$\alpha_s(m_\tau^2) = 0.330 \pm 0.025, \tag{51}$$

the $\overline{\mathrm{MS}}$ charm quark mass and the gluon condesate were determined to be

$$\bar{m}(\bar{m}^2) = 1.275 \pm 0.015\,\mathrm{GeV},$$

$$\left\langle \frac{\alpha_s}{\pi} G^2 \right\rangle = 0.009 \pm 0.007\,\mathrm{GeV}^4. \tag{52}$$

The error in (52) roughly comprises as 50% theoretical (uncertainty in α_s and the normalization scale) and 50% experimental (mainly the error of the J/ψ electronic decay width). The numbers in (52) were obtained disregarding the contribution of the G^3 operator. The account of the G^3 term, when $\langle G^3\rangle$ was taken using the dilute instanton gas model with $\rho_c = 0.5\,\mathrm{fm}$, shifts (52) to

$$\left\langle \frac{\alpha_s}{\pi} G^2 \right\rangle = 0.011 \pm 0.009\,\mathrm{GeV}^4. \tag{53}$$

The value (53) may be compared with the recently found [19] limitation on the gluon condensate from hadronic τ-decay data:

$$\left\langle \frac{\alpha_s}{\pi} G^2 \right\rangle = 0.006 \pm 0.012\,\mathrm{GeV}^4. \tag{54}$$

Equations (53) and (54) are compatible and are obtained from independent sources. So, with some courage, we can average them and get

$$\left\langle \frac{\alpha_s}{\pi} G^2 \right\rangle_{\mathrm{av}} = 0.0085 \pm 0.0075\,\mathrm{GeV}^4. \tag{55}$$

After such averaging we come back to (52).

We can formulate our final conclusion about the gluon condensate value as follows. The values of the gluon condensate two times (or more) larger than the SVZ value (2) are certainly excluded. Unfortunately our analysis does not allow us to exclude zero values of the gluon condensate. In this respect the improvement of the experimental precision of the $J/\psi \to e^+e^-$ width would be helpful. Based on the condensate limitation (54) and the value of α_s (51), the J/ψ electronic decay width $\Gamma_{J/\psi\to ee}$ was predicted theoretically:

$$\Gamma^{\mathrm{theor}}_{J/\psi\to ee} = 4.9 \pm 0.8\,\mathrm{keV}, \tag{56}$$

to be compared with the experimental value $5.26 \pm 0.37\,\mathrm{keV}$. Such a good coincidence ones more demonstrates the effectiveness of the QCD sum rule approach.

Acknowledgements. The authors thank A.I. Vainstein and K.G. Chetyrkin for fruitful discussions. The research described in this publication was made possible in part by Award No. RP2-2247 of the U.S. Civilian Research and Development Foundation for Independent States of the Former Soviet Union (CRDF), by the Russian Found of Basic Research grant 00-02-17808 and INTAS grant 2000, project 587.

Appendix: Numerical values of the moments

We list here the numerical values of the perturbative moments $\bar{M}^{(0,1,2)}$, the condensate contribution $\bar{M}^{(G,0,1)}$ in the $\overline{\mathrm{MS}}$ scheme computed by (37) and the $\langle G^3\rangle$ condensate contribution $M^{(G3)}$ (47) for $n = 1 \ldots 20$ and $Q^2/(4\bar{m}^2) = 0, 1, 2$. For dimensionful values we put $4\bar{m}^2 = 1$ here, so that the leading term $\bar{M}^{(0)}$ and the ratios $\bar{M}^{(G,0)}/\bar{M}^{(0)}$, $\bar{M}^{(G3)}/\bar{M}^{(0)}$ should be divided by $(4\bar{m}^2)^n$ and $(4\bar{m}^2)^2$, $(4\bar{m}^2)^3$ respectively for a particular mass $\bar{m}$.

Table 2. Moments at $Q^2 = 0$

n	$\bar{M}_n^{(0)}$	$\bar{M}_n^{(1)}/\bar{M}_n^{(0)}$	$\bar{M}_n^{(2)}/\bar{M}_n^{(0)}$	$\bar{M}_n^{(G,0)}/\bar{M}_n^{(0)}$	$\bar{M}_n^{(G,1)}/\bar{M}_n^{(G,0)}$	$\bar{M}_n^{(G3)}/\bar{M}_n^{(0)}$
1	0.8	2.394	2.384	−15.04	2.477	0.056
2	0.3429	2.427	6.11	−58.49	1.054	0.826
3	0.2032	1.917	6.115	−143.6	−0.484	4.003
4	0.1385	1.1	4.402	−283.4	−2.107	12.76
5	0.1023	0.078	2.162	−491.3	−3.798	32.21
6	7.9565×10^{-2}	−1.092	0.213	−780.3	−5.545	69.81
7	6.4187×10^{-2}	−2.375	−0.836	−1164.	−7.337	135.9
8	5.3207×10^{-2}	−3.75	−0.514	−1654.	−9.17	243.9
9	4.5043×10^{-2}	−5.199	1.559	−2266.	−11.04	411.2
10	3.8776×10^{-2}	−6.711	5.698	−3011.	−12.94	659.1
11	3.3841×10^{-2}	−8.277	12.17	−3903.	−14.86	1014.
12	2.9872×10^{-2}	−9.89	21.19	−4955.	−16.81	1506.
13	2.6624×10^{-2}	−11.54	32.98	−6181.	−18.78	2172.
14	2.3924×10^{-2}	−13.23	47.69	−7593.	−20.77	3055.
15	2.1653×10^{-2}	−14.96	65.49	−9204.	−22.78	4204.
16	1.9719×10^{-2}	−16.71	86.51	-1.103×10^4	−24.81	5673.
17	1.8058×10^{-2}	−18.49	110.9	-1.308×10^4	−26.85	7526.
18	1.6617×10^{-2}	−20.3	138.7	-1.537×10^4	−28.91	9834.
19	1.5359×10^{-2}	−22.13	170.1	-1.791×10^4	−30.98	1.268×10^4
20	1.4252×10^{-2}	−23.98	205.2	-2.072×10^4	−33.07	1.614×10^4

Table 3. Moments at $Q^2 = 4\bar{m}^2$

n	$\bar{M}_n^{(0)}$	$\bar{M}_n^{(1)}/\bar{M}_n^{(0)}$	$\bar{M}_n^{(2)}/\bar{M}_n^{(0)}$	$\bar{M}_n^{(G,0)}/\bar{M}_n^{(0)}$	$\bar{M}_n^{(G,1)}/\bar{M}_n^{(G,0)}$	$\bar{M}_n^{(G3)}/\bar{M}_n^{(0)}$
1	0.4348	2.235	−0.307	−2.816	4.532	−0.02
2	9.7902×10^{-2}	2.64	4.407	−10.19	4.03	−0.058
3	2.9985×10^{-2}	2.709	6.752	−23.8	3.455	−0.082
4	1.047×10^{-2}	2.588	7.653	−45.32	2.825	−0.014
5	3.9365×10^{-3}	2.34	7.582	−76.4	2.15	0.279
6	1.5529×10^{-3}	1.999	6.85	−118.7	1.438	1.004
7	6.3364×10^{-4}	1.587	5.683	−173.9	0.697	2.452
8	2.6515×10^{-4}	1.118	4.253	−243.5	−0.071	5.015
9	1.1314×10^{-4}	0.601	2.7	−329.4	−0.862	9.197
10	4.9032×10^{-5}	0.045	1.136	−433.	−1.673	15.63
11	2.1523×10^{-5}	−0.546	−0.343	−556.1	−2.501	25.09
12	9.5483×10^{-6}	−1.167	−1.656	−700.3	−3.346	38.5
13	4.2743×10^{-6}	−1.815	−2.732	−867.3	−4.205	56.96
14	1.9283×10^{-6}	−2.486	−3.508	−1059.	−5.078	81.75
15	8.7574×10^{-7}	−3.178	−3.93	−1276.	−5.962	114.4
16	4.0007×10^{-7}	−3.89	−3.948	−1521.	−6.858	156.4
17	1.8372×10^{-7}	−4.62	−3.518	−1795.	−7.764	209.9
18	8.4756×10^{-8}	−5.365	−2.599	−2101.	−8.68	277.
19	3.9264×10^{-8}	−6.126	−1.154	−2439.	−9.605	360.
20	1.8257×10^{-8}	−6.9	0.85	−2811.	−10.54	461.7

Table 4. Moments at $Q^2 = 8\bar{m}^2$

n	$\bar{M}_n^{(0)}$	$\bar{M}_n^{(1)}/\bar{M}_n^{(0)}$	$\bar{M}_n^{(2)}/\bar{M}_n^{(0)}$	$\bar{M}_n^{(G,0)}/\bar{M}_n^{(0)}$	$\bar{M}_n^{(G,1)}/\bar{M}_n^{(G,0)}$	$\bar{M}_n^{(G3)}/\bar{M}_n^{(0)}$
1	0.3005	2.073	−2.016	−1.098	5.002	-8.936×10^{-3}
2	4.6172×10^{-2}	2.531	2.453	−3.825	4.762	−0.03
3	9.589×10^{-3}	2.734	5.208	−8.691	4.468	−0.064
4	2.2613×10^{-3}	2.792	6.909	−16.2	4.131	−0.105
5	5.7274×10^{-4}	2.753	7.853	−26.84	3.761	−0.14
6	1.5191×10^{-4}	2.643	8.229	−41.11	3.364	−0.147
7	4.1621×10^{-5}	2.478	8.167	−59.5	2.942	−0.094
8	1.1682×10^{-5}	2.27	7.769	−82.51	2.501	0.066
9	3.3404×10^{-6}	2.025	7.113	−110.6	2.042	0.393
10	9.6957×10^{-7}	1.749	6.264	−144.3	1.568	0.963
11	2.8488×10^{-7}	1.447	5.276	−184.1	1.08	1.871
12	8.4559×10^{-8}	1.122	4.195	−230.4	0.579	3.233
13	2.5317×10^{-8}	0.776	3.061	−283.9	0.068	5.186
14	7.6361×10^{-9}	0.412	1.909	−344.8	−0.455	7.89
15	2.3181×10^{-9}	0.031	0.77	−413.8	−0.986	11.53
16	7.0768×10^{-10}	−0.364	−0.33	−491.3	−1.527	16.33
17	2.1713×10^{-10}	−0.773	−1.365	−577.8	−2.075	22.52
18	6.6914×10^{-11}	−1.195	−2.313	−673.9	−2.631	30.38
19	2.0704×10^{-11}	−1.628	−3.153	−779.9	−3.194	40.21
20	6.429×10^{-12}	−2.072	−3.867	−896.4	−3.764	52.36

References

1. M.A. Shifman, A.I. Vainstein, V.I. Zakharov, Nucl. Phys. B **147**, 385 (1979); 448
2. L.J. Reinders, H.R. Rubinstein, S. Yazaki, Nucl. Phys. B **186**, 109 (1981)
3. S. Narison, QCD spectral sum rules (World Scientific, 1989); Phys. Lett. B **387**, 162 (1996)
4. V.A. Novikov, M.A. Shifman, A.I. Vainstein, M.B. Voloshin, V.I. Zakharov, Nucl. Phys. B **237**, 525 (1984)
5. S.I. Eidelman, L.M. Kurdadze, A.I. Vainstein, Phys. Lett B **82**, 278 (1979)
6. K.J. Miller, M.G. Olsson, Phys. Rev. D **25**, 1247 (1982)
7. R.A. Bertlmann, Nucl. Phys. B **204**, 387 (1982)
8. V.N. Baier, Yu.F. Pinelis, Phys. Lett. B **116**, 179 (1982); Nucl. Phys. B **229**, 29 (1983)
9. G. Launer, S. Narison, R. Tarrach, Z. Phys. C **26**, 433 (1984)
10. R.A. Bertlmann, C.A. Domingues, M. Loewe, M. Perrottet, E. de Rafael, Z. Phys. C **39**, 231 (1988)
11. P.A. Baikov, V.A. Ilyin, V.A. Smirnov, Phys. Atom. Nucl. **56**, 1527 (1993)
12. D.J. Broadhurst, P.A. Baikov, V.A. Ilyin, J. Fleischer, O.V. Tarasov, V.A. Smirnov, Phys. Lett. B **329**, 103 (1994)
13. B.V. Geshkenbein, Phys. Atom. Nucl. **59**, 289 (1996)
14. S.N. Nikolaev, A.V. Radyushkin, JETP Lett. **37**, 526 (1982)
15. M. Jamin, A. Pich, Nucl. Phys. B **507**, 334 (1997)
16. M. Eidemuller, M. Jamin, Phys. Lett. B **498**, 203 (2001)
17. J.H. Kuhn, M. Steinhauser, Nucl. Phys. B **619**, 588 (2001)
18. S. Eidelman, E. Jergenlehner, A.L. Kataev, O. Veretin, Phys. Lett. B **454**, 369 (1999)
19. B.V. Geshkenbein, B.L. Ioffe, K.N. Zyablyuk, Phys. Rev. D **64**, 093009 (2001)
20. K. Hagiwara et al. (Particle Data Group), Phys. Rev. D **66**, 010001 (2002)
21. J.Z. Bai et al. (BES Collaboration), Phys. Rev. Lett. **88**, 101802 (2002)
22. V.B. Berestetski, I.Ya. Pomeranchuk, Sov. Phys. JETF **29**, 864 (1955)
23. J. Schwinger, Particles, sources and fields, Vol. 2 (Addison-Wesley Publ., 1973)
24. A.H. Hoang, J.H. Kuhn, T. Teubner, Nucl. Phys. B **452**, 173 (1995)
25. K.G. Chetyrkin, J.H. Kuhn, M. Steinhauser, Nucl. Phys. B **482**, 213 (1996)
26. K.G. Chetyrkin, A.H. Hoang, J.H. Kuhn, M. Steinhauser, T. Teubner, Eur. Phys. J. C **2**, 137 (1998)
27. K.G. Chetyrkin, R. Harlander, J.H. Kuhn, M. Steinhauser, Nucl. Phys. B **503**, 339 (1997)
28. N. Gray, D.J. Broadhurst, W. Grafe, K. Schilcher, Z. Phys. C **48**, 573 (1990)
29. K. Melnikov, T. van Ritbergen, Phys. Lett. B **482**, 99 (2000); K.G. Chetyrkin, M. Steinhauser, Nucl. Phys. B **573**, 617 (2000)
30. S.N. Nikolaev, A.V. Radyushkin, Sov. J. Nucl. Phys. **39**, 91 (1984)
31. V.A. Novikov, M.A. Shifman, A.I. Vainstein, V.I. Zakharov, Phys. Lett. B **86**, 347 (1979)
32. T. Shafer, E.V. Shuryak, Rev. Mod. Phys. **70**, 323 (1998)
33. B.L. Ioffe, A.V. Samsonov, Phys. At. Nucl. **63**, 1448 (2000)
34. V.A. Novikov et al., Phys. Rep. **41**, 1 (1978)
35. M.B. Voloshin, Nucl. Phys. B **154**, 365 (1979); Int. J. Mod. Phys. A **10**, 2865 (1995)
36. J.H. Kuhn, A.A. Penin, A.A. Pivovarov, Nucl. Phys. B **534**, 356 (1998)
37. V.A. Khoze, M.A. Shifman, Sov. Phys. Usp. **26**, 387 (1983)
38. L. Landau, E, Lifshitz, Quantum mechanics: Non-relativistic theory (Pergamon Press, 1977)
39. E. Eichten et al., Phys. Rev. D **21**, 203 (1980)